JOURNAL OF BACTERIOLOGY, Feb. 1997, p. 1068–1076 Vol. 179, No. 4
0021-9193/97/$04.00+0

AUT1, a Gene Essential for Autophagocytosis in the Yeast *Saccharomyces cerevisiae*

MARTIN SCHLUMPBERGER, ELKE SCHAEFFELER, MICHAEL STRAUB, MONIKA BREDSCHNEIDER, DIETER H. WOLF, AND MICHAEL THUMM*

Institut für Biochemie, Universität Stuttgart, D-70550 Stuttgart, Germany

Received 31 October 1996/Accepted 3 December 1996

Autophagocytosis is a starvation-induced process responsible for transport of cytoplasmic proteins to the vacuole. In *Saccharomyces cerevisiae*, autophagy is characterized by the phenotypic appearance of autophagic vesicles inside the vacuole of strains deficient in proteinase yscB. The *AUT1* gene, essential for autophagy, was isolated by complementation of the sporulation deficiency of a diploid *aut1-1* mutant strain by a yeast genomic library and characterized. *AUT1* is located on the right arm of chromosome XIV, 10 kb from the centromere, and encodes a protein of 310 amino acids, with an estimated molecular weight of 36 kDa. Cells carrying a chromosomal deletion of *AUT1* are defective in the starvation-induced bulk flow transport of cytoplasmic proteins to the vacuole. *aut1* null mutant strains are completely viable but show decreased survival rates during starvation. Homozygous Δ*aut1* diploid cells fail to sporulate. The selective cytoplasm-to-vacuole transport of aminopeptidase I is blocked in logarithmically growing and in starved Δ*aut1* cells. Deletion of the *AUT1* gene had no obvious influence on secretion, fluid phase endocytosis, or vacuolar protein sorting. This supports the idea of autophagocytosis as being a novel route transporting proteins from the cytoplasm to the vacuole.

Cells have developed sophisticated mechanisms to adapt to changes in the nutritional environment. One major process enabling cells to survive periods of nitrogen deprivation is degradation of large amounts of intracellular proteins. Eukaryotic cells contain two major systems for protein degradation, the proteasome and the lysosome (18, 21). While the proteasome seems to be responsible for the breakdown of regulated and short-lived proteins (17), the starvation-induced proteolytic breakdown is dependent mainly on the lysosome. An interesting question is how cytosolic proteins enter the lysosomal (vacuolar) lumen.

Morphological studies preferentially done with mammalian cells have demonstrated that this protein uptake process is due mainly to unselective bulk flow autophagocytosis (for reviews, see references 8 and 34). Detailed electron microscopic studies supported the idea that cytoplasm containing double or multilayered early autophagosomes are most likely formed from parts of the endoplasmic reticulum (9, 13, 45). These vesicles are further maturing to late autophagosomes and autolysosomes (10, 24, 26).

Another, more selective mechanism for vacuolar protein uptake during nutrient deprivation, based on a KFERQ-related pentapeptide motif, was proposed by Dice (6).

As a simple eukaryotic model organism which is easily amenable to genetic manipulations, we used the yeast *Saccharomyces cerevisiae* to study gene products involved in the uptake process of proteins from the cytoplasm into the vacuole. Under nitrogen starvation conditions in *Saccharomyces cerevisiae*, nearly half of the total cellular protein content is degraded during a 24-h period. More than 80% of this degradation takes place inside the vacuole, the counterpart of the mammalian lysosome (40). Following the concomitant uptake of several cytosolic enzymes into the vacuole, the unselective nature of protein entry into the vacuole in this organism was demonstrated (11). A detailed microscopic analysis showed the appearance of autophagic vesicles inside the vacuole, when cells with defects in the vacuolar endoproteinases yscA or yscB are subject to starvation (37, 39). The accumulation of these vesicles can also be induced by incubating the cells in nitrogen-deficient media in the presence of the proteinase yscB inhibitor phenylmethylsulfonyl fluoride (PMSF) (39, 41). By indirect immunofluorescence microscopy, it has been shown that fatty acid synthase, a cytoplasmic marker protein, is localized inside these autophagic vesicles (41).

For genetic dissection of autophagocytosis, we isolated autophagocytosis mutants, i.e., mutants defective in the autophagic process (41). These *aut* mutants are defective in the breakdown of a cytoplasmic marker protein, fatty acid synthase, whose degradation during starvation was shown to be dependent mainly on the action of the vacuolar proteinases. Furthermore, *aut* mutants are unable to accumulate autophagic vesicles in the vacuolar lumen during periods of nitrogen starvation.

Another set of mutants (*apg*) with a defect in autophagocytosis was isolated due to their reduced ability to survive during starvation (44).

Here we report the isolation and sequencing of the *AUT1* gene, shown to be essential for the autophagocytotic process. Chromosomal deletion of *AUT1* does not influence growth on rich media but leads to a reduced survival rate of the mutant cells during periods of nitrogen starvation. Autophagocytosis seems to be an essential prerequisite for sporulation. Homozygously deleted *aut1* diploids are defective in the formation of asci. The block of autophagocytosis in chromosomal *aut1*-deleted cells has no significant influence on endocytosis (29), secretion (31, 33), or vacuolar biogenesis (5, 38). Most recently, a phenotypic and genetic overlap of autophagocytosis and the selective import of aminopeptidase I from the cytoplasm into the vacuole (16, 20) has been found (15). We found Δ*aut1* mutant strains to be impaired in the maturation of the precursor of aminopeptidase I. Our findings support the idea that autophagocytosis constitutes a new route of protein transport from the cytoplasm to the vacuole.

* Corresponding author. Mailing address: Institut für Biochemie, Universität Stuttgart, Pfaffenwaldring 55, D-70550 Stuttgart, Germany. Fax: 49 711 6854392. E-mail: thumm@po.uni-stuttgart.de.

TABLE 1. List of strains

Strain	Genotype	Reference or source
WCG4a	*MATa his3-11,15 leu2-3,112 ura3*	41
WCGAa	*MATα his3-11,15 leu2-3,112 ura3 ade2ΔA*	This work
YMTAa	*MATa his3-11,15 leu2-3,112 ura3 pra1Δ::HIS3*	41
YMS5α	*MATα his3-11,15 leu2-3,112 ura3 aut1Δ1::URA3*	This work
YMS6a	*MATa his3-11,15 leu2-3,112 ura3 ade2Δ1 aut1Δ1::ADE2*	This work
YMS7a	*MATa his3-11,15 leu2-3,112 ura3 ade2Δ1 aut1Δ1::URA3*	This work
YMS8α	*MATα his3-11,15 leu2-3,112 ura3 aut1Δ1::URA3 pra1Δ::HIS3*	This work
DYY101	*MATα leu2-3,112 ura3-52 his3-Δ200 trp1-Δ901 ade2-101 suc2-Δ9 GAL ape1::LEU2*	20
RH932	*MATa ura3 leu2 bar1 end2*	H. Riezman

MATERIALS AND METHODS

Chemicals. PMSF was purchased from Serva, Heidelberg, Germany; zymolyase 100T was from Seikagaku Kyogo, Tokyo, Japan; lucifer yellow and quinacrine were from Sigma, Deisenhofen, Germany; goat anti-rabbit antibodies labeled with horseradish peroxidase were from Medac, Hamburg, Germany; L-[^{35}S]methionine, α-^{35}S-dATP, and tissue solubilizer NCS-II were from Amersham-Buchler, Braunschweig, Germany. All other chemicals were from Sigma or Roth (Karlsruhe, Germany), and all were of analytical grade.

Synthetic oligonucleotides were from Eurogentec, Ougrée, Belgium, and MWG Biotech, Ebersberg, Germany

Antibodies. Antibodies directed against proteinases yscA, yscB, and yscY as well as fatty acid synthase are described elsewhere (11, 12, 25); antibodies against aminopeptidase I were generously provided by D. J. Klionsky (20).

Media. Yeast strains were grown either in complete liquid medium YPD (1% yeast extract, 2% peptone, 2% glucose) or complete minimal dropout medium CM (consisting of 0.67% yeast nitrogen base [without amino acids] and 2% glucose and supplemented with adenine, uracil, and amino acids) as described previously (1). For starvation or sporulation, cells were incubated in 1% potassium acetate.

Strains. For strains used, see Table 1. Strain WCGAa was obtained by chromosomal deletion of the *ADE2* gene in WCG4a with a 2.3-kb *Bam*HI fragment from pPL131. Strain YMS5α was made by transforming a 3.5-kb *Xba*I fragment from pAUT1Δ1::URA3 into the genome of WCG4α; strain YMS6a was made by transforming a 4.6-kb *Bam*HI-*Sac*I fragment from pAUT1Δ1::ADE2 into WCGAa; and YMS7a was made by transforming a 3.5-kb *Xba*I fragment from pAUT1Δ1::URA3 into WCG4a. YMS8 was obtained from a cross of YMS5 and YMTA. The *end2* mutant strain RH932 was kindly provided by H. Riezman.

Plasmids. Standard DNA cloning and manipulation was done as described before (1). For DNA sequencing, we used the T7 DNA sequencing kit obtained from Pharmacia, Freiburg, Germany. Plasmid pPL131 used for chromosomal deletion was a gift from P. Ljungdahl, Stockholm, Sweden.

Plasmid pRSp8 containing the *S. cerevisiae* genomic DNA including the *AUT1* locus was selected from a YCplac111-based library (5a). For subcloning of a genomic fragment containing the functional *AUT1* gene, a 3.3-kb *Xba*I fragment was isolated from pRSp8 and cloned into the *Xba*I site of pRS315, pRS316, pRS306 (36), or pRS426 (4) to obtain plasmids pRS315/AUT1, pRS316/AUT1, pRS306/AUT1, and pRS426/AUT1, respectively. For chromosomal deletion of *AUT1*, a 0.9-kb *Bgl*II-*Nco*I fragment was removed from pRS315/AUT1 and replaced by a 1.1-kb *URA3* fragment, yielding plasmid pAUT1Δ1::URA3. In a second approach, a 2.2-kb fragment containing the functional *ADE2* marker was used to get pAUT1Δ1::ADE2.

Screening procedure. The *ade2* deletion allele from pPL131 was chromosomally introduced into an *aut1-1* mutant strain, and the resulting strain was crossed with an *aut1-1 ADE2* mutant strain of the opposite mating type. The resulting diploid strain was transformed with yeast genomic libraries based on the *CEN LEU2* shuttle vector YCplac111 (5a) or the 2μm *URA3* shuttle vector YEp24 (3), and complementation of the nonsporulating phenotype of the diploid was searched for. The resulting colonies were washed from the plates, diluted into 1% potassium acetate at an optical density at 600 nm (OD_{600}) of approximately 10, and incubated for 4 to 6 days at room temperature for sporulation. From 100 μl of sporulated cells, random spores were prepared by digestion with 0.1 mg of zymolyase 100T in 5 ml of sterile water, followed by the addition of 5 ml of 1.5% Nonidet P-40 solution and sonification. Thereafter, cells were washed and plated on selective media. The ratio between red (*ade2*) and white colonies (*ADE2* or *ade2*/*ADE2*) was always near 1:1, indicating that very few diploid cells survived this procedure. Red colonies were picked and tested for the ability to accumulate autophagic vesicles upon starvation in the presence of PMSF as described previously (41).

Microscopy. Microscopic observations were done with a Zeiss Axioskop MC100 microscope. Visualization of autophagic vesicles inside the vacuole was done as described before (41). Vacuolar acidification was examined by observing accumulation of the fluorescent dye quinacrine inside the vacuole by standard procedures (30). Endocytosis was examined as described previously (7) by accumulation of lucifer yellow. Staining with MDY-64 was done as proposed by Molecular Probes Europe BV, Leiden, The Netherlands.

Cell fractionation. Spheroplast formation, lysis, and preparation of vacuole-enriched and cytosolic fractions were performed as described by Harding et al. (15), except that cells were starved for 24 h at room temperature before spheroplast formation and preincubation in the presence of dithiothreitol was done for 30 min. Whole spheroplasts were harvested and washed at 1,000 × *g*.

Electrophoresis and immunoblotting. Cell extracts were prepared as described before (11), samples were separated by sodium dodecyl sulfate-polyacrylamide gel electrophoresis (10 or 12% acrylamide [23]) and blotted onto nitrocellulose membranes (43). To prevent unspecific binding of antibodies to nitrocellulose, membranes were incubated in PBS-T buffer (0.1% Tween 20, 100 mM NaCl, 20 mM potassium phosphate [pH 7.5]) containing 10% nonfat milk for at least 2 h.

For immunodetection, primary antisera against proteinases yscA and yscB were used at a dilution rate of 1:5,000, and antisera against carboxypeptidase yscY, aminopeptidase I, and fatty acid synthase were used at a dilution of 1:10,000 in PBS-T for at least 1 h. After washing three times in PBS-T and incubation with peroxidase-conjugated goat anti-rabbit secondary antibody at a dilution of 1:5,000 for 1 h, membranes were washed and the bands were visualized with the enhanced chemiluminescence detection kit provided by Amersham-Buchler.

Protein turnover. Cells were grown in 10 ml labeling medium (consisting of 0.17% yeast nitrogen base [without amino acids and ammonium sulfate], 2% proline, and 2% glucose and supplemented with the appropriate auxotrophic nutrients) at 30°C to approximately 5×10^7 cells/ml. In the last 14 h of growth, 3.7 MBq of L-[^{35}S]methionine was added to the culture. After labeling, the cells were collected by centrifugation, washed three times with starvation medium, resuspended in starvation medium containing 10 mM nonradioactive methionine, and further incubated at 30°C. At the indicated times, 1-ml samples were taken, mixed with 100 μl of 110% trichloroacetic acid, and incubated on ice for at least 4 h. For determination of the released acid-soluble radioactivity, the samples were centrifuged for 5 min at 14,000 × g. Nine hundred microliters of the supernatant was mixed with 5 ml of liquid scintillation mixture. For determination of the total incorporated radioactivity, the pellets of the 0-h samples were washed five times with starvation medium containing 10% trichloroacetic acid and two times with ethanol-ether (1:1). The pellets were air dried and dissolved in 1 ml of NCS-II–H_2O (9:1) at 40°C. Nine hundred microliters of the solution was mixed with 5 ml of liquid scintillator. Radioactivity was determined with a Wallace 1410 liquid scintillation counter (Pharmacia).

Survival during starvation. Cells of different strains were grown to equal ODs in YPD medium, harvested, and resuspended in 1% potassium acetate to an OD_{600} of 0.02 to 0.05. Every 24 h, samples were taken, diluted, and plated, and the number of colonies growing was determined. The relative survival rate compared with the number of colonies recovering after the first 24 h of starvation was calculated.

Secretion of invertase. Secretion of invertase was assayed as described previously (27), without shifting the cells to 37°C.

RESULTS

The *aut1-1* mutant strain FIM35 obtained by ethyl methanesulfonate mutagenesis (41) was backcrossed four times with the wild-type strain WCG4α. Seventy-nine tetrads were analyzed for the phenotypic appearance of autophagic vesicles in the vacuole in the presence of PMSF. All tetrads showed a 2:2 segregation of vesicle accumulation. This demonstrates the existence of a recessive, single point mutation responsible for the *aut1-1* phenotype. From the segregation pattern of the *aut1-1* mutation and the centromere-linked auxotrophic marker *trp1* (data not shown), the genetic distance (35) of

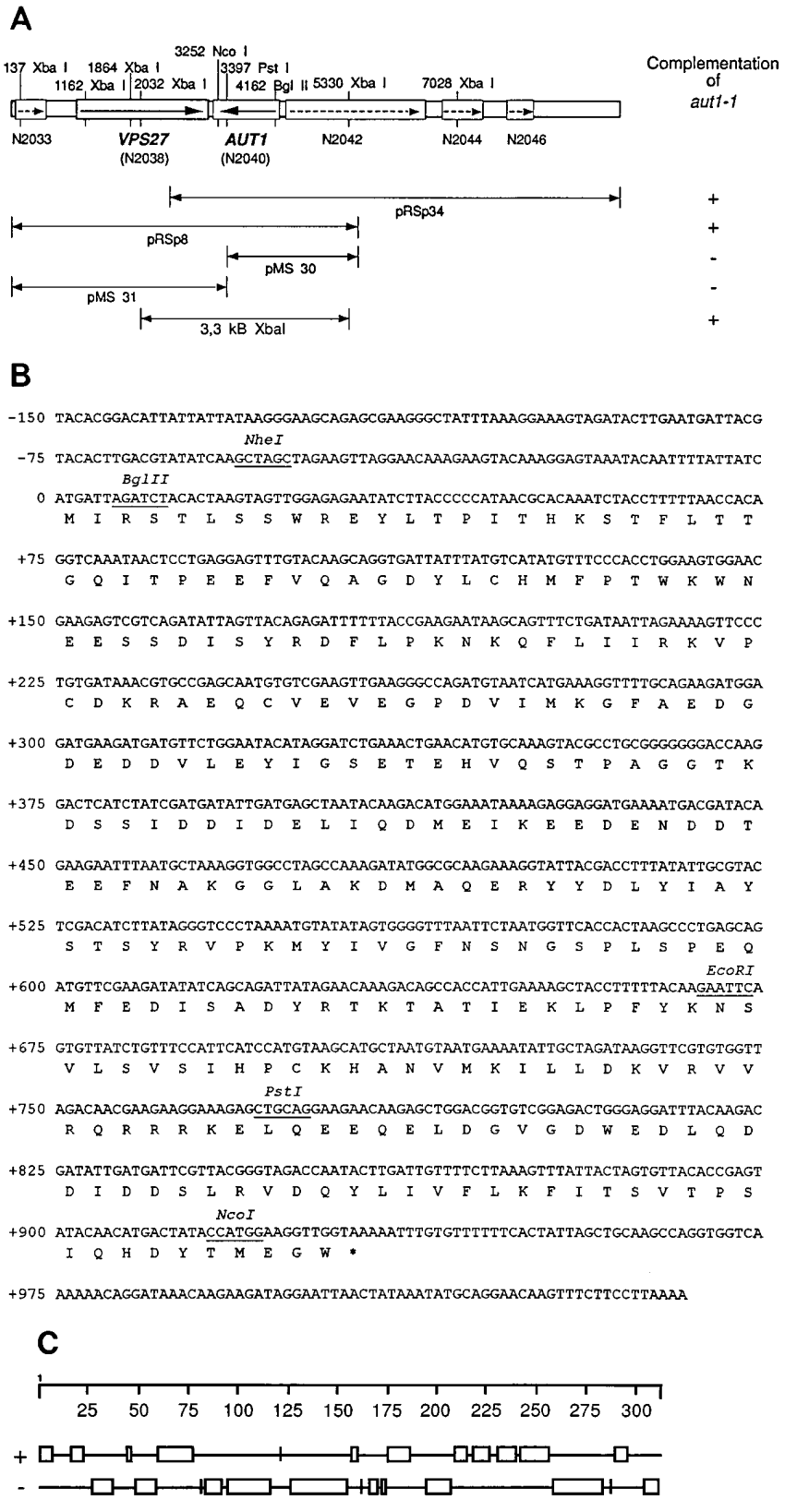

FIG. 1. (A) Part of the genomic DNA fragment SCN201952 surrounding the *AUT1* gene. The chromosome XIV centromere sequence is located near position −7300. Also shown are the genomic fragments obtained from the library plasmids pRSp8 and pRSp34, the two subclones made from pRSp8, and the fragment used for subcloning of the *AUT1* gene. (B) Sequence of the *AUT1* gene. The nucleotide sequence of *AUT1* is identical to the published sequence of ORF *N2040*. Amino acids are shown in a single-letter code. Recognition sites of several commonly used DNA restriction enzymes are indicated. (C) Clusters of positively and negatively charged amino acid residues within Aut1p.

AUT1 to the centromere was calculated to be 7.6 cM. A localization in direct neighborhood to *TRP1* did not seem likely from these data.

Isolation of the *AUT1* gene. In our attempt to isolate the *AUT1* gene, we took advantage of the drastically reduced sporulation frequency of a homozygous *aut1-1*/*aut1-1* diploid mutant strain. After transformation of this diploid strain with a plasmid-encoded yeast chromosomal library, predominantly those cells bearing a plasmid-borne *AUT1* wild-type gene should be able to form asci. Most of the nonsporulated diploid cells were killed by following the established random spore protocol (1). The use of a heterozygous *ade2*/*ADE2* diploid strain allowed the rapid recognition of ascospores after this procedure. Only *ade2* haploid ascospores exhibited the typical red pigment. A plasmid-encoded *AUT1* gene should rescue not only the sporulation defect but also the defect in the autophagic pathway seen in an *aut1-1* mutant strain. Therefore, the red colonies were further tested for restoration of their ability to accumulate autophagic vesicles inside the vacuole during a 4-h starvation period on nitrogen-free medium in the presence of PMSF.

In a typical experiment, batches of 3,000 clones transformed with the genomic library were pooled, sporulated, and subjected to the random spore procedure. After spreading on plates, 20 to 40 red colonies were checked from each batch for their ability to accumulate autophagic vesicles. By use of the centromeric YCplac111 genomic library, 45,000 colonies were analyzed in total. In one batch, five positive colonies were detected, and the respective plasmids were rescued. All plasmids were found to be identical and contained a 5.5-kb genomic insert (pRSp8) (Fig. 1A).

In a similar approach, by use of an overexpressing high-copy Yep24-derived genomic library, 15,000 transformands were screened in five batches. Four positive colonies containing identical plasmids (pRSp34) with a 7.5-kb genomic insert were found. Partial sequencing of the genomic inserts of pRSp8 and pRSp34 localized both of them to chromosome XIV, genomic fragment SCN201952 (Fig. 1A) (47). The genomic fragment SCN201952 is located on the right arm of chromosome XIV, directly flanking the centromere, which is in good agreement with the calculated genetic distance of the *aut1-1* locus 7.6 cM from the centromere. The only complete open reading frame (ORF) present in both of the plasmids pRSp8 and pRSp34 was the ORF *N2040*. A 3.3-kb *Xba*I fragment from pRSp8 containing only ORF *N2040* was subcloned into the vector pRS315 and found to be capable to restore the vesicle accumulation defect of the *aut1-1* mutant strain. As expected, two subclones starting at the unique *Pst*I site inside *N2040* were unable to complement the *aut1-1* mutation (Fig. 1A). The described 3.3-kb *Xba*I fragment was chromosomally integrated in an *aut1-1* mutant, and the resulting strain was crossed with a wild-type strain. All ascospores exhibited a wild-type phenotype. This confirmed that the isolated ORF *N2040* was indeed identical to *AUT1*. Resequencing of *AUT1* did not uncover any discrepancies with the known sequence (47) in the databases (Fig. 1B). *AUT1* encodes a protein with 310 amino acids and a calculated molecular size of 36 kDa. The *AUT1* gene product Aut1p seems to be quite hydrophilic with clusters of charged amino acids (Fig. 1C) and a predicted isoelectric point of 4.4. A stretch of 23 amino acids (residues 130 to 152) seems to fulfill the definition given by Realini et al. (28) for KEKE motifs, although there is only one K present. KEKE motifs have been proposed to be involved in the assembly of proteins into larger complexes. The Aut1p contains no obvious transmembrane domains. The Aut1p shows no significant homologies to other proteins of known function in the databases.

Chromosomal deletion of *AUT1*. Chromosomal *aut1* null mutant strains were constructed by deleting the *AUT1* coding region between the *Bgl*II and *Nco*I restriction sites (Fig. 1B) and inserting the *URA3* or *ADE2* gene, respectively, as a selectable marker. The correct gene replacement was confirmed by Southern hybridization and PCR (data not shown).

The resulting strains YMS5 (*aut1*Δ*1::URA3*) and YMS6 (*aut1*Δ*1::ADE2*) were viable and did not show any growth phenotypes at 10, 30, or at 37°C (data not shown). Vacuolar morphology was checked with Nomarski optics (Fig. 2A) and the vacuolar membrane dye MDY-64 (Fig. 2B). Δ*aut1* cells exhibited a clearly visible vacuole, which appeared smaller than wild-type vacuoles. The membranes of autophagic vesicles accumulating inside the vacuoles of starved *pra1*-deficient cells could also be stained with MDY-64 (Fig. 2B). Quinacrine, a dye routinely used to detect the acidification of the vacuole (30), accumulated normally inside the vacuoles of Δ*aut1* cells (Fig. 2C).

As expected, *aut1* null mutant strains showed a block in the autophagic pathway, demonstrated by their inability to accumulate autophagic vesicles inside the vacuole during starvation for nitrogen in the presence of the proteinase yscB inhibitor PMSF (Fig. 2A). For further confirmation of a defect in the uptake of cytoplasmic proteins into the vacuolar lumen of these strains, we checked the subcellular localization of a cytoplasmic protein, fatty acid synthase, after a 24-h starvation period for nitrogen. For cell fractionation, spheroplasted cells were hypotonically lysed without affecting the integrity of the vacuole. Thereafter, cytoplasmic and vacuolar enriched fractions were isolated in a centrifugation step (15). To prevent the degradation of cytoplasmic proteins inside the vacuole, strains defective in proteinase yscA (*pra1*/*pep4*) were used for this experiment. As a control for proper vacuolar enrichment, the localization of the resident vacuolar proteinase yscB was also checked (Fig. 3). As shown in Fig. 3A, lane P, in an *AUT1* wild-type, *pra1*-deficient strain, significant amounts of both subunits of the cytoplasmic fatty acid synthase can be detected in the vacuolar enriched fraction by immunoblotting, whereas in the *aut1*/*pra1* null mutant strain, no fatty acid synthase is localized to the vacuole (Fig. 3B, lane P).

Demonstration that not only the uptake of a single cytoplasmic protein into the vacuole but also the unspecific bulk flow of proteins to the vacuole is affected in *aut1*-deleted cells was brought about by determining the overall protein turnover rate. All cellular proteins were radiolabeled in growing cells with L-[^{35}S]methionine. Thereafter, cells were shifted to a nitrogen-free, nonradioactive starvation medium. After precipitating nondegraded proteins with trichloroacetic acid, the amount of acid-soluble small peptides generated by the action of the intracellular proteinases was determined (Fig. 4). Under these conditions, a wild-type strain exhibited an initial protein breakdown rate of 1.8% per h. The block of vacuolar proteolysis in a *pra1*-deficient strain reduces this rate to 18% of the level of a wild-type strain; the residual proteolysis rate is mainly due to the action of nonvacuolar proteinases, most likely, the cytosolic and nuclear proteasome (40). A nearly identical reduction of protein degradation to 18% of that of the wild type was detected in an *aut1* null mutant strain (Fig. 4). This gives a strong indication for a block of unselective protein uptake into the vacuole due to the defect in Aut1p.

Vacuolar proteolysis is most prominent in cells starving for nitrogen, and proteinase yscA-deficient cells cannot survive extended times of starvation (40, 46). We therefore measured the ability of haploid Δ*aut1* cells to survive a starvation period (Fig. 5). Similar to a *pra1*-deficient strain, Δ*aut1* cells exhibited a significantly reduced survival rate. After prolonged periods of

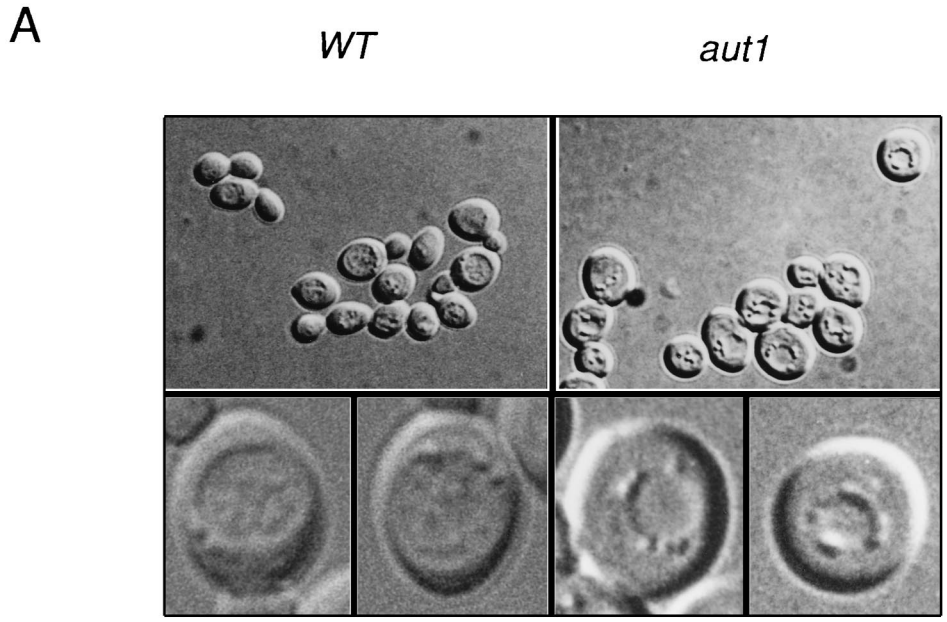
A
WT
aut1

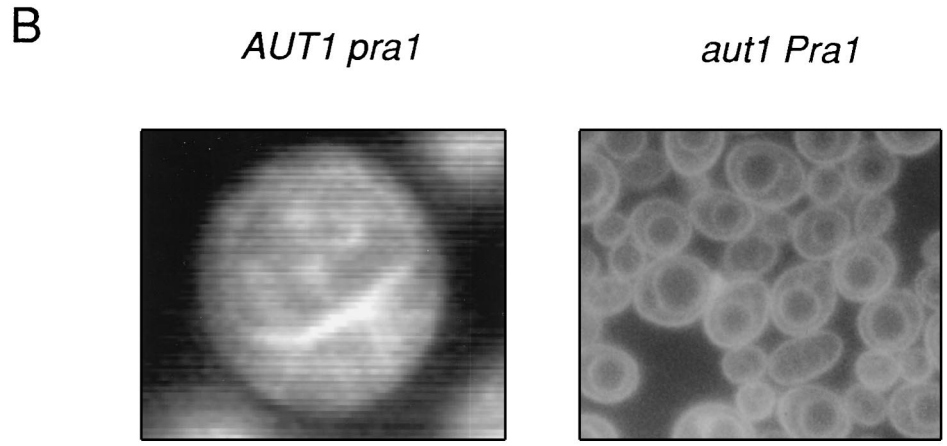
B
AUT1 pra1
aut1 Pra1

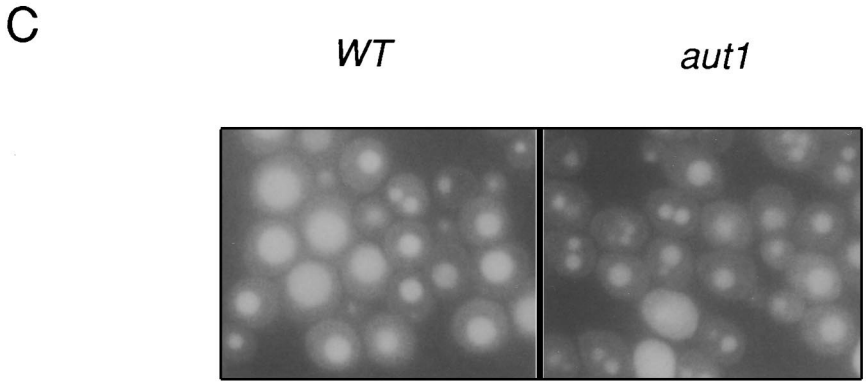
C
WT
aut1

FIG. 2. (A) Accumulation of autophagic vesicles in the vacuolar lumen during starvation in the presence of PMSF is blocked in *aut1* deletion strains. After 4 h of starvation, the vacuole of wild-type strain WCG4a is filled with vesicles (WT). Under the same conditions, no vesicles can be observed in vacuoles of the *aut1* null mutant strain YMS5 (*aut1*). (B) Vacuolar morphology. Morphology of vesicles after starvation for 4 h stained with the fluorescent dye MDY-64. Strain YMTA, carrying the *pra1* null allele, shows normal vacuolar morphology. Autophagic vesicles accumulated under these conditions are also stained by the dye (figure produced with Zeiss video imaging system). The vacuole of strain YMS6 (*aut1*Δ*1::ADE2*) is morphologically similar to vacuoles of strain YMTA except that no vesicles are accumulating (figure produced with a Zeiss Axioskop MC100 microscope). (C) pH-dependent accumulation of the fluorescent dye quinacrine in the vacuolar lumen. Vacuolar staining of Δ*aut1* cells (right) is not distinguishable from that of wild type (left), indicating that acidification of the vacuole occurs normally in the mutant cells.

starvation, the survival rate of the Δ*aut1* strain was even lower than that of a *pra1*-deficient strain (Fig. 5).

Diploid cells respond to nutrient limitation by the differentiation process of sporulation and the formation of asci. Sporulation frequency was determined either by counting the asci under the microscope or by using *ade2*/*ADE2* heterozygous diploids and counting the number of red colonies formed after a random spore procedure. For calculation of sporulation frequencies, the viability of cells after sporulation was tested and only viable cells were taken into consideration to exclude any influence from mutant cells dying of starvation. Wild-type and heterozygous *AUT1*/Δ*aut1* diploids showed normal sporulation rates under various conditions (data not shown), whereas homozygous Δ*aut1*/Δ*aut1* cells completely failed to sporulate. From several million viable diploid cells, we were unable to recover any haploid colonies or observe any asci microscopically (data not shown).

Overlap with other vesicle transport processes. We elucidated a potential overlap of autophagocytosis and other vesicle-mediated processes by checking the influence of a chromosomal *aut1* deletion on several other protein transport processes.

Biogenesis of the vacuole. The correct sorting of soluble vacuolar proteinases to the vacuole is a good indication of undisturbed vacuolar biogenesis. An analysis of the steady-state levels of the proteinases yscA and yscB and carboxypeptidase yscY by immunoblotting showed only the mature forms of these enzymes in Δ*aut1* cells after starvation (Fig. 6A) as well as in growing cells (data not shown). Recently, a more rigid kinetic pulse chase analysis of carboxypeptidase yscY maturation showed a wild-type-like sorting of this enzyme to the vacuole in an *aut1-1* mutant strain (15).

Secretion. The efficiency of secretion was measured (Fig. 6B) by use of invertase as a well-known marker enzyme for secretion (32). The appearance of enzymatically active, extracellular invertase after induction of the enzyme by glucose deprivation was examined. There was no significant alteration in the time course of invertase secretion visible in an *aut1*-deficient strain as compared with that of a wild-type strain (Fig. 6B).

Endocytosis. In contrast to endocytosis-defective mutants, the ability of *aut1* null mutant cells to take up lucifer yellow into the vacuole by fluid-phase endocytosis (7) was not affected (Fig. 6C).

Cytoplasm-to-vacuole targeting of aminopeptidase I. Aminopeptidase I was shown to be synthesized as a precursor in the cytoplasm, from where it is targeted directly to the vacuole without the detour through the secretory pathway. In the vacuole, the enzyme undergoes maturation by proteinase yscB (20). Cells deleted in the chromosomal *aut1* gene are defective in maturation of preaminopeptidase I (Fig. 7). In crude extracts of logarithmically growing cells or cells starved for 4 h, no mature aminopeptidase I could be recognized (Fig. 7, lanes 4). A centromeric plasmid carrying the *AUT1* gene almost completely cured this defect in logarithmically growing as well as in starved cells (Fig. 7, lanes 5). A small amount of preaminopeptidase I is still visible. Overexpression of *AUT1* from a 2μ plasmid did not further reduce the amount of aminopeptidase I precursor (lanes 6).

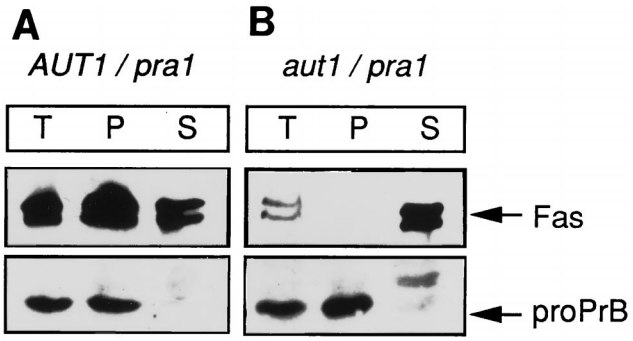

FIG. 3. Cell fractionation. Cellular extracts of total spheroplasts (T), a vacuolar enriched pellet (P), and a cytosolic enriched supernatant (S) fraction were prepared as described after 24 h of starvation, separated by sodium dodecyl sulfate-polyacrylamide gel electrophoresis, blotted, and probed with antibodies directed against the α- and β-subunits of fatty acid synthase and proteinase yscB. (A) The *pra1* deletion strain shows accumulation of fatty acid synthase together with the vacuolar marker yscB in the vacuole-enriched fraction (P) after starvation. (B) In a *pra1*/*aut1* double mutant strain under identical conditions, no fatty acid synthase is found in the fraction containing proteinase yscB, thereby demonstrating the block in autophagic transport due to deletion of the *AUT1* gene.

DISCUSSION

The autophagic process of cytoplasmic protein uptake and delivery to the lysosome (vacuole) is not yet understood at the molecular level. To gain some understanding of this process, we followed a genetic approach with the model eukaryote *S. cerevisiae*. Analysis of an *aut1-1* mutant strain, isolated by its inability to degrade a cytosolic marker protein and its inability to accumulate autophagic vesicles in the vacuole, sheds some first light on this process.

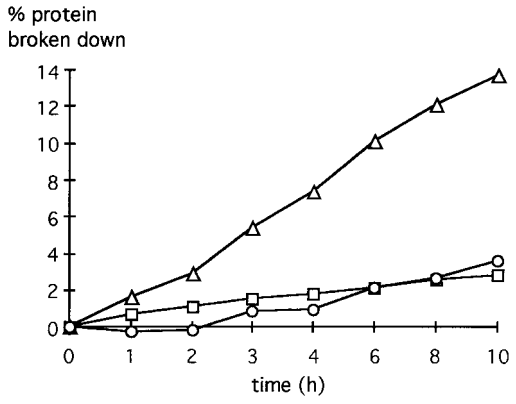

FIG. 4. Degradation of total cellular proteins during starvation. The *pra1* deletion strain YMTA (□) showed drastically reduced turnover rates compared with that of the wild-type strain WCG4a (△). The same reduction in degradation could be observed in the *aut1* null mutant YMS6 (○).

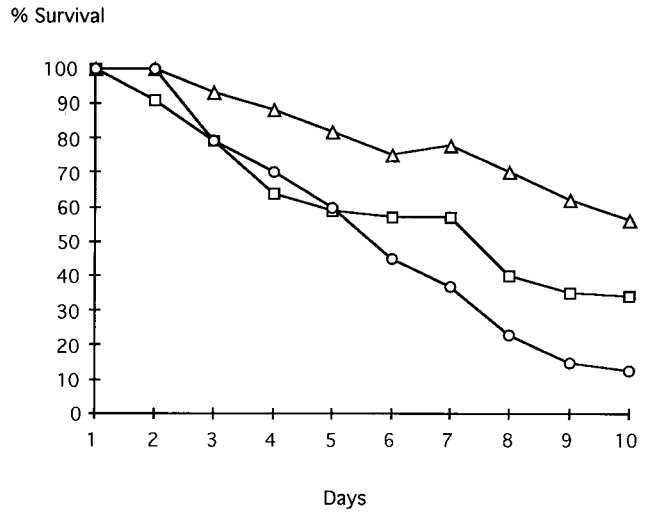

FIG. 5. Survival during starvation in 1% potassium acetate (at an OD_{600} of 0.02 to 0.05). Like the *pra1* mutant strain YMTA (□), the *aut1* mutant YMS5 (○) showed a drastically reduced survival rate as compared with that of the wild-type strain WCG4a (△).

By use of the drastically reduced sporulation frequency of a homozygous *aut1-1*/*aut1-1* diploid strain, we developed a new screening procedure which allows the rapid isolation of genes related to the autophagic process. This led us to the isolation of the *AUT1* gene, which was sequenced and found to be identical to ORF *N2040* on the right arm of chromosome XIV. The *AUT1* gene encodes a protein of 310 amino acids that contains no obvious transmembrane domain. A search for homologs of Aut1p in the protein databases identified no significant similarities to other proteins of known function. One striking feature of Aut1p is the high content of charged amino acids.

We constructed chromosomal *aut1* null mutant strains and confirmed the complete block of autophagocytosis in these strains by demonstrating the absence of any autophagic vesicles in the vacuolar lumen during a starvation period for nitrogen in the presence of PMSF. In mammalian tissues, autophagocytosis is well known as a starvation-induced transport process of cytoplasmic proteins into the lysosome. We therefore routinely used nitrogen starvation conditions with only 1% potassium acetate as the culture medium to fully induce the autophagic pathway. We performed cell fractionation experiments with *pra1*-deficient cells to prevent the degradation of proteins in the vacuolar lumen. In cells wild type for autophagocytosis, the cytosolic fatty acid synthase can be found in the vacuolar fraction after starvation as a result of the autophagic process. The lack of fatty acid synthase in the vacuolar enriched fraction of Δ*aut1* cells confirmed the inability of these cells to import cytosolic proteins into the vacuole.

Under starvation conditions in a strain wild type for proteinase and autophagocytosis, 40% of all cellular proteins were shown to be subject to vacuolar proteolysis during a 24-h period (40). We measured the overall protein breakdown rates in Δ*aut1* cells. Similar to a proteinase yscA-deficient strain, which is impaired in almost the complete protein breakdown inside the vacuole (19, 40, 46), an *aut1* null mutant strain had a reduced proteolysis rate of 0.32% of all proteins per h compared with the rate of 1.8% per h found in a wild-type strain. This reduction very much supports the idea of autophagocytosis as being an unspecific bulk flow protein transport pathway

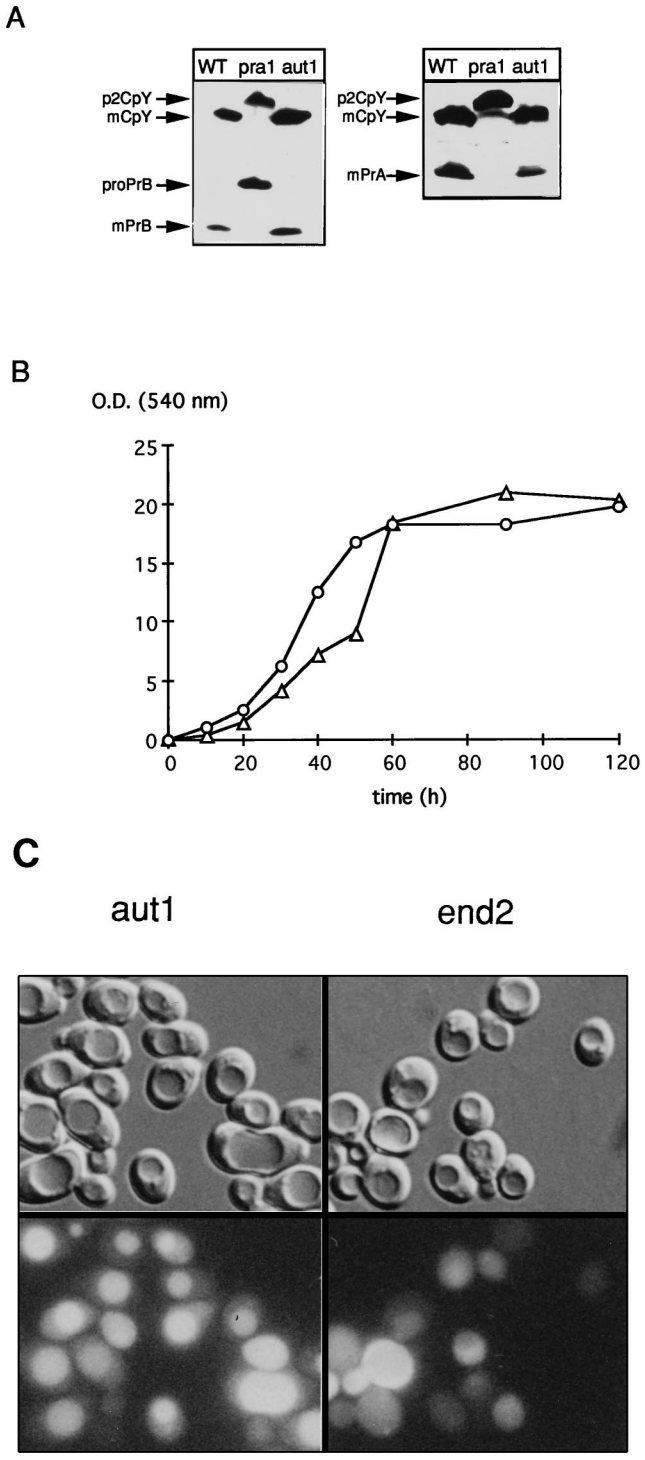

FIG. 6. Overlap of autophagocytosis with other vesicle transport processes. (A) Vacuolar proteinases yscA, yscB, and yscY are fully matured in *aut1* deletion strains. All strains were starved for 4 h in acetate medium. The *pra1* mutant strain YMTA showed only the precursor forms of proteinase yscB (proPrB) and carboxypeptidase Y (p2CpY) and no proteinase yscA. From the *aut1* mutant, as from the wild-type strain, only the mature forms (mPrB, mCpY, and mPrA) are recovered. (B) Secretion of invertase occurred at the wild-type level in *aut1* mutant strains. In the supernatants of wild-type strain WCG4a (△) and *aut1* deletion strain YMS5 (○), invertase activities increase with similar kinetics after induction. (C) Accumulation of lucifer yellow was normal in *aut1* mutants. Results for *aut1* null mutant strain YMS6, visualized by Nomarski optics and fluorescence, with the *end2* mutant strain RH932 as a negative control are shown. Under identical conditions, lucifer yellow is enriched in the vacuoles of YMS6 but not in RH932. Vacuolar staining of YMS6 is undistinguishable from that of the wild type.

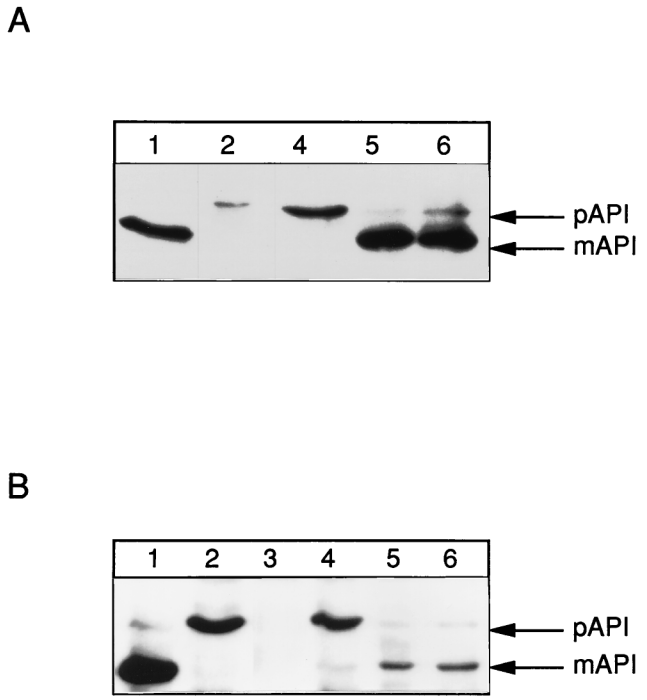

FIG. 7. Maturation of aminopeptidase I. Cell extracts were examined from wild-type strains (lanes 1), *pra1* mutant strains (lanes 2), or from the *aut1* mutant strain YMS6 with plasmids pRS316 (lanes 4), pRS316/*AUT1* (lanes 5) or pRS426/*AUT1* (lanes 6). The extract in lane 3 of both panels was derived from an aminopeptidase I deletion strain. (A) Samples collected from logarithmically growing cells. (B) Samples collected after 4 h of starvation. In both cases, maturation of aminopeptidase I is prevented by deletion of *PEP4* or *AUT1*

to the vacuole. This is also in good agreement with previous findings that different cytoplasmic proteins enter the vacuole at the same rate (11, 22).

The availability of a chromosomal *aut1* null mutant strain allowed a detailed study of the importance of autophagy for cellular function. There was no influence visible of an *aut1* deletion on cellular viability on rich media like YPD. As compared with that of the wild type, growth was also unchanged at 10, 30, and 37°C. This demonstrates that autophagocytosis is not essential for the cell in rich media, containing the proper amount of amino acids and utilizable nitrogen. However, autophagocytosis plays a prominent role in the adaption of cells to nutrient limitation conditions. *aut1*-deficient cells showed a drastically reduced ability to survive if nitrogen was omitted from the medium. The differentiation process of sporulation of diploid cells, another starvation-linked process, was also severely affected. Homozygous *aut1*-deleted diploids are unable to form asci.

The overlap of autophagocytosis with other vesicular transport processes like vacuolar biogenesis, secretion, or endocytosis is still an open question. A lot of work has been done with mammalian cells to answer this question (for a review, see reference 8). A connection between endocytosis and autophagocytosis has been demonstrated in mammalian cells by the appearance of endocytosed material in autophagic vacuoles (14, 42), but the major route seems to be fusion of autophagic vesicles with preexisting lysosomes (24). In *S. cerevisiae*, an ultrastructural analysis showed double membrane-layered autophagosome-like structures in the cytosol. Sometimes, the outer membrane of these structures has been found in continuity with the vacuolar membrane (2). This proposes a membrane fusion event that could explain the appearance of single membrane-surrounded vesicles in the vacuolar lumen (37, 39).

Interestingly, we found that the membranes of autophagic vesicles, which accumulate inside vacuoles, could be stained with MDY-64, a dye routinely used to stain the vacuolar membrane. This might be a hint that the membranes of the autophagic vesicles in the vacuolar lumen to some extent resemble the vacuolar membrane.

We checked the effect of a block of autophagocytosis caused by an *aut1* deletion on vacuolar morphology by using light microscopy with Nomarski optics and detected a wild-type-like vacuole with a slightly reduced size. Staining with the vacuolar membrane marker MDY-64 and vacuolar acidification probed with quinacrine (30) showed no difference between the *aut1* deletion mutant and a wild-type strain. A steady-state analysis of the maturation of the proteinases yscA, yscB, and yscY, as well as a kinetic analysis of carboxypeptidase yscY sorting to the vacuole, showed no defect in the vacuolar protein sorting pathway. The time course of invertase secretion and the uptake of lucifer yellow by fluid phase endocytosis were wild type like. Taken together, these results suggest that Aut1p plays no essential function for other vesicle-mediated processes. This supports the idea that autophagocytosis constitutes a novel route to the vacuole, with no generally essential function for endocytosis and vacuolar biogenesis.

The action of Aut1p has been found to be essential for the selective vacuolar uptake of aminopeptidase I in logarithmically growing and in starving cells (15). This beautifully illustrates the occurrence of autophagocytosis not only during starvation but also in logarithmically growing cells in rich media. Indeed, Teichert et al. have found vacuolar proteolysis responsible for 30 to 40% of the total proteolysis rate in logarithmically growing cells (40).

Aut1p may function as a soluble cytosolic factor in the autophagic process by interacting with other specific proteins. This idea is supported by the existence of clusters of charged amino acids in the Aut1p. Such clusters have been proposed to be involved in the association of proteins (28). In an attempt to localize the Aut1p, we created epitope-tagged versions of the protein by inserting the HA epitope (hemagglutinin from *Haemophilus influenzae*) into the protein. Unfortunately, all constructs created to date were unable to complement the defects seen in an *aut1*-deleted strain and were therefore not useful to localize the Aut1p in the cells. Further studies to localize the Aut1p in the cells and to shed light on its precise function in the autophagic process are under way.

ACKNOWLEDGMENTS

We thank Daniel J. Klionsky for generously providing antibodies directed against aminopeptidase I and the aminopeptidase I deletion strain, Howard Riezman for the *end2* mutant strain, and Per Ljungdahl for his *ADE2* deletion constructs. The YCplac111 genomic library was a gift from F. Cvrckova.

This work was supported by DFG, Bonn, Germany (grant Wo210/12-1), and the Fonds der Chemischen Industrie, Frankfurt, Germany.

REFERENCES

1. **Ausubel, F. M., R. Brent, R. E. Kingston, and D. D. Moore.** 1987. Current protocols in molecular biology. Greene Publishing Associates, New York, N.Y.
2. **Baba, M., K. Takeshige, N. Baba, and Y. Ohsumi.** 1994. Ultrastructural analysis of the autophagic process in yeast: detection of autophagosomes and their characterization. J. Cell. Biol. **124:**903–913.
3. **Carlson, M., and D. Botstein.** 1982. Two differentially regulated mRNAs with different 5′ ends encode secreted with intracellular forms of yeast invertase. Cell **28:**145–154.
4. **Christianson, T. W., R. S. Sikorsky, M. Dante, J. H. Shero, and P. Hieter.** 1992. Multifunctional yeast high-copy-number shuttle vectors. Gene **110:** 119–122.

5. **Conibear, E., and T. H. Stevens.** 1995. Vacuolar biogenesis in yeast: sorting out the sorting proteins. Cell **83:**513–516.

5a. **Cvrckova, F.** 1991. Unpublished data.

6. **Dice, J. F.** 1990. Peptide sequences that target cytosolic proteins for lysosomal proteolysis. Trends Biochem. Sci. **15:**305–309.

7. **Dulic, V., M. Egerton, I. Elguindi, S. Raths, B. Singer, and H. Riezman.** 1991. Yeast endocytosis assays. Methods Enzymol. **194:**697–710.

8. **Dunn, W. J.** 1994. Autophagy and related mechanisms of lysosome-mediated protein degradation. Trends Cell Biol. **4:**139–143.

9. **Dunn, W. J.** 1990. Studies on the mechanisms of autophagy: formation of the autophagic vacuole. J. Cell Biol. **110:**1923–1933.

10. **Dunn, W. J.** 1990. Studies on the mechanisms of autophagy: maturation of the autophagic vacuole. J. Cell Biol. **110:**1935–1945.

11. **Egner, R., M. Thumm, M. Straub, A. Simeon, H. J. Schuller, and D. H. Wolf.** 1993. Tracing intracellular proteolytic pathways. Proteolysis of fatty acid synthase and other cytoplasmic proteins in the yeast *Saccharomyces cerevisiae*. J. Biol. Chem. **268:**27269–27276.

12. **Finger, A., M. Knop, and D. H. Wolf.** 1993. Analysis of two mutated vacuolar proteins reveals a degradation pathway in the endoplasmic reticulum or a related compartment of yeast. Eur. J. Biochem. **218:**565–574.

13. **Furuno, K., T. Ishikawa, K. Akasaki, S. Lee, Y. Nishimura, H. Tsuji, M. Himeno, and K. Kato.** 1990. Immunocytochemical study of the surrounding envelope of autophagic vacuoles in cultured rat hepatocytes. Exp. Cell Res. **189:**261–268.

14. **Gordon, P. B., H. Hoyvik, and P. O. Seglen.** 1992. Prelysosomal and lysosomal connections between autophagy and endocytosis. Biochem. J. **283:**361–369.

15. **Harding, T. M., A. Hefner-Gravink, M. Thumm, and D. J. Klionsky.** 1996. Genetic and phenotypic overlap between autophagy and the cytoplasm to vacuole targeting pathway. J. Biol. Chem. **271:**17621–17624.

16. **Harding, T. M., K. A. Morano, S. V. Scott, and D. J. Klionsky.** 1995. Isolation and characterization of yeast mutants in the cytoplasm to vacuole protein targeting pathway. J. Cell. Biol. **131:**591–602.

17. **Hilt, W., and D. H. Wolf.** 1996. Proteasomes destruction as a programme. Trends Biochem. Sci. **21:**96–101.

18. **Hilt, W., and D. H. Wolf.** 1992. Stress-induced proteolysis in yeast. Mol. Microbiol. **6:**2437–2442.

19. **Jones, E. W.** 1991. Three proteolytic systems in the yeast *Saccharomyces cerevisiae*. J. Biol. Chem. **266:**7963–7966.

20. **Klionsky, D. J., R. Cueva, and D. S. Yaver.** 1992. Aminopeptidase I of *Saccharomyces cerevisiae* is localized to the vacuole independent of the secretory pathway. J. Cell Biol. **119:**287–299.

21. **Knop, M., H. H. Schiffer, S. Rupp, and D. H. Wolf.** 1993. Vacuolar/lysosomal proteolysis: proteases, substrates, mechanisms. Curr. Opin. Cell Biol. **5:**990–996.

22. **Kopitz, J., G. O. Kisen, P. B. Gordon, P. Bohley, and P. O. Seglen.** 1990. Nonselective autophagy of cytosolic enzymes by isolated rat hepatocytes. J. Cell Biol. **111:**941–953.

23. **Laemmli, U. K.** 1970. Cleavage of structural proteins during the assembly of the head of bacteriophage T4. Nature **227:**680–685.

24. **Lawrence, B. P., and W. J. Brown.** 1992. Autophagic vacuoles rapidly fuse with pre-existing lysosomes in cultured hepatocytes. J. Cell Sci. **102:**515–526.

25. **Mechler, B., M. Muller, H. Muller, F. Meussdoerffer, and D. H. Wolf.** 1982. In vivo biosynthesis of the vacuolar proteinases A and B in the yeast *Saccharomyces cerevisiae*. J. Biol. Chem. **257:**11203–11206.

26. **Rabouille, C., G. J. Strous, J. D. Crapo, H. J. Geuze, and J. W. Slot.** 1993. The differential degradation of two cytosolic proteins as a tool to monitor autophagy in hepatocytes by immunocytochemistry. J. Cell Biol. **120:**897–908.

27. **Raths, S., J. Rohrer, F. Crausaz, and H. Riezman.** 1993. end3 and end4: two mutants defective in receptor-mediated and fluid-phase endocytosis in *Saccharomyces cerevisiae*. J. Cell Biol. **120:**55–65.

28. **Realini, C., S. W. Rogers, and M. Rechsteiner.** 1994. KEKE motifs. Proposed roles in protein-protein association and presentation of peptides by MHC class I receptors. FEBS Lett. **348:**109–113.

29. **Riezman, H.** 1993. Yeast endocytosis. Trends Cell Biol. **3:**273–277.

30. **Roberts, C. J., C. K. Raymond, C. T. Yamahiro, and T. H. Stevens.** 1991. Methods for studying the yeast vacuole. Methods Enzymol. **194:**644–661.

31. **Schekman, R.** 1992. Genetic and biochemical analysis of vesicular traffic in yeast. Curr. Opin. Cell Biol. **4:**587–592.

32. **Schekman, R., B. Esmon, S. Ferro-Novick, C. Field, and P. Novick.** 1983. Yeast secretory mutants: isolation and characterization. Methods Enzymol. **96:**802–815.

33. **Schekman, R., and L. Orci.** 1996. Coat proteins and vesicle budding. Science **271:**1526–1533.

34. **Seglen, P. O., and P. Bohley.** 1992. Autophagy and other vacuolar protein degradation mechanisms. Experientia **48:**158–172.

35. **Sherman, F., and P. Wakem.** 1991. Mapping yeast genes. Methods Enzymol. **194:**38–57.

36. **Sikorski, R. S., and P. Hieter.** 1989. A system of shuttle vectors and yeast host strains designed for efficient manipulation of DNA in *Saccharomyces cerevisiae*. Genetics **122:**19–27.

37. **Simeon, A., I. van der Klei, M. Veenhuis, and D. H. Wolf.** 1992. Ubiquitin, a central component of selective cytoplasmic proteolysis, is linked to proteins residing at the locus of non-selective proteolysis, the vacuole. FEBS Lett. **301:**231–235.

38. **Stack, J. H., B. Horazdovsky, and S. D. Emr.** 1995. Receptor-mediated protein sorting to the vacuole in yeast: roles for a protein kinase, a lipid kinase and GTP-binding protein. Annu. Rev. Cell Dev. Biol. **11:**1–33.

39. **Takeshige, K., M. Baba, S. Tsuboi, T. Noda, and Y. Ohsumi.** 1992. Autophagy in yeast demonstrated with proteinase-deficient mutants and conditions for its induction. J. Cell Biol. **119:**301–311.

40. **Teichert, U., B. Mechler, H. Muller, and D. H. Wolf.** 1989. Lysosomal (vacuolar) proteinases of yeast are essential catalysts for protein degradation, differentiation, and cell survival. J. Biol. Chem. **264:**16037–16045.

41. **Thumm, M., R. Egner, B. Koch, M. Schlumpberger, M. Straub, M. Veenhuis, and D. H. Wolf.** 1994. Isolation of autophagocytosis mutants of *Saccharomyces cerevisiae*. FEBS Lett. **349:**275–280.

42. **Tooze, J., M. Hollinshead, T. Ludwig, K. Howell, B. Hoflack, and H. Kern.** 1990. In exocrine pancreas, the basolateral endocytic pathway converges with the autophagic pathway immediately after the early endosome. J. Cell Biol. **111:**329–345.

43. **Towbin, H., T. Staehelin, and J. Gordon.** 1979. Electrophoretic transfer of proteins from polyacrylamide gels to nitrocellulose sheets: procedure and some applications. Proc. Natl. Acad. Sci. USA **76:**4350–4354.

44. **Tsukada, M., and Y. Ohsumi.** 1993. Isolation and characterization of autophagy-defective mutants of *Saccharomyces cerevisiae*. FEBS Lett. **333:**169–174.

45. **Ueno, T., D. Muno, and E. Kominami.** 1991. Membrane markers of endoplasmic reticulum preserved in autophagic vacuolar membranes isolated from leupeptin-administered rat liver. J. Biol. Chem. **266:**18995–18999.

46. **van den Hazel, H. B., M. C. Kielland-Brandt, and J. R. Winther.** 1996. Review: biosynthesis and function of yeast vacuolar proteases. Yeast **12:**1–16.

47. **Verhasselt, P., R. Aert, M. Voet, and G. Volckaert.** 1994. Twelve open reading frames revealed in the 23.6 kb segment flanking the centromere on the *Saccharomyces cerevisiae* chromosome XIV right arm. Yeast **10:**1355–1361.